Genes & Diseases (2023) 10, 239–253

Available online at www.sciencedirect.com

ScienceDirect

journal homepage: www.keaipublishing.com/en/journals/genes-diseases

FULL LENGTH ARTICLE

Desulfovibrio desulfuricans aggravates atherosclerosis by enhancing intestinal permeability and endothelial TLR4/NF-κB pathway in *Apoe*$^{-/-}$ mice

Kun Zhang [a,1], Xian Qin [a,1], Juhui Qiu [a,,1], Tong Sun [b], Kai Qu [a], Ahmad Ud Din [a], Wenhua Yan [a], Tianhan Li [a], Yidan Chen [a], Wei Gu [c], Xiancai Rao [d], Guixue Wang [a,*]**

[a] *Key Laboratory for Biorheological Science and Technology of Ministry of Education, State and Local Joint Engineering Laboratory for Vascular Implants, College of Bioengineering, Chongqing University, Chongqing 400044, China*
[b] *College of Information and Management Sciences, Henan Agricultural University, Zhengzhou, Henan 450046, China*
[c] *School of Medicine, Chongqing University, Chongqing 400030, China*
[d] *Department of Microbiology, College of Basic Medical Sciences, Army Medical University (Third Military Medical University), Chongqing 400037, China*

Received 11 May 2021; received in revised form 27 August 2021; accepted 23 September 2021
Available online 16 October 2021

KEYWORDS
Atherosclerosis;
Desulfovibrio desulfuricans;
Gut microbiota;
Linear discriminant analysis;
TAK-242

Abstract It is increasingly aware that gut microbiota is closely associated with atherosclerosis. However, which and how specific gut bacteria regulate the progression of atherosclerosis is still poorly understood. In this study, modified linear discriminant analysis was performed in comparing the gut microbiota structures of atherosclerotic and non-atherosclerotic mice, and *Desulfovibrio desulfuricans* (*D. desulfuricans*) was found to be associated with atherosclerosis. *D. desulfuricans*-treated *Apoe*$^{-/-}$ mice showed significantly aggravated atherosclerosis. The proatherogenic effect of *D. desulfuricans* was attributed to its ability to increase intestinal permeability and subsequent raise in the transit of lipopolysaccharide (LPS) from the intestine to the bloodstream. Excessive LPS in the blood can elicit local and systemic inflammation and activate Toll-like receptor 4 (TLR4)/nuclear factor-κB (NF-κB) signaling of endothelial cells.

* Corresponding author.
** Corresponding author.
E-mail addresses: jhqiu@cqu.edu.cn (J. Qiu), wanggx@cqu.edu.cn (G. Wang).
Peer review under responsibility of Chongqing Medical University.
[1] These authors contributed equally to this work.

https://doi.org/10.1016/j.gendis.2021.09.007

TAK-242, a specific inhibitor of TLR4, can ameliorate the development of *D. desulfuricans*-induced atherosclerosis by blocking the LPS-induced activation of TLR4/NF-κB signaling.

Introduction

Atherosclerosis, a chronic inflammatory disease, is considered a major cause of vascular death (such as myocardial infarction and stroke) worldwide.[1–3] Given that growing evidence has revealed that the gut microbiota plays an important role in human health and diseases, including atherosclerosis,[4–9] gut microbiota—host interaction has attracted significant interest. The gut microbiota functions like an endocrine organ that can modulate the development of atherosclerosis by producing functional molecules, altering intestinal permeability, and regulating partial and systemic inflammation.

Sulfate-reducing bacteria (SRB) colonize the guts of ~50% of humans[10,11] and exacerbate gastrointestinal diseases by generating hydrogen sulfide and inhibiting the production of butyrate of *Firmicutes*.[12] *Desulfovibrio desulfuricans* (*D. desulfuricans*) is an anaerobe that grows rapidly in anaerobic habitats[13,14] and is the predominant SRB in human colonic microbiota.[14] *D. desulfuricans* is enriched in patients with ulcerative colitis[14,15] and type 2 diabetes[16] and implicated in inflammatory bowel diseases, liver abscesses, and appendicitis.[17] However, the correlation between *D. desulfuricans* and atherosclerosis has not been reported.

Linear discriminant analysis (LDA) is a classical statistical approach for dimensionality reduction and classification and has been used in extracting features through different linear transformations.[18] In this study, modified LDA (M-LDA) indicates that *D. desulfuricans* greatly contributes to the process of atherosclerosis. Then, we investigated the effects of *D. desulfuricans* on the atherosclerosis of *Apoe*$^{-/-}$ mice. Results showed that the abundance of *D. desulfuricans* increased in *Apoe*$^{-/-}$ mice subjected to a high-fat-diet. The administration of *D. desulfuricans* can aggravate the development of atherosclerotic lesions in *Apoe*$^{-/-}$ mice. We further explored the mechanisms of the deleterious effect of gut-residing *D. desulfuricans*.

Materials and methods

Animals

Apoe$^{-/-}$ mice in the C57BL/6 background were obtained from the Third Military Medical University (SCXK-PLA-20170005) and housed in a specific pathogen-free animal facility. All of the animal care and experimental protocols were carried out with the approval of the Laboratory Animal Welfare and Ethics Committee of the Third Military Medical University (SYXK-PLA-20170005). Eight-week-old male *Apoe*$^{-/-}$ mice were fed with normal chow or subjected to high-fat-diet (Cat #: D12108C) *ad libitum* under a strict 12 h light/12 h dark cycle for 10 weeks. The mice were randomly divided into six groups: (a) mice in the control group were fed with normal chow diet and treated with PBS (NCD); (b) mice in the control group were subjected to a high-fat-diet and treated with PBS (HFD + PBS); (c) high-fat-diet mice were treated with live *D. desulfuricans* (HFD + Des); (d) high-fat-diet mice were treated with heat-killed *D. desulfuricans* (HFD + hk-Des); (e) high-fat-diet mice treated with live *D. desulfuricans* and injected with Toll-like receptor 4 (TLR4) inhibitor TAK-242 (HFD + Des + inhi); (f) high-fat-diet mice were treated with PBS and injected with TAK-242 (HFD + inhi). At the end of the experiment, mice were euthanized by intravenous injection of a lethal dose of pentobarbital sodium (100 mg kg^{-1}), and their organ tissues were removed and collected for further biochemical analysis.

Screening of atherosclerosis related bacteria

Feces from 12 atherosclerotic mice (AS group, *Apoe*$^{-/-}$ mice treated with high-fat-diet for 8 weeks) and 12 non-atherosclerotic mice (CK group, *Apoe*$^{-/-}$ mice treated with normal chow diet for 8 weeks) were collected. DNA was extracted from fecal matter with Qiagen DNeasy PowerSoil kit.[19] The V3—V4 region of the 16S rRNA gene was sequenced using an Illumina Miseq platform (Illumina Inc., CHN) according to the manufacturer's protocol. The sequences for all operational taxonomic units (OTUs) of each sample were subjected to the Ribosomal Database Project Classifier for taxonomic assignment with a bootstrap cutoff of 97%. The principal coordinate analysis (PCoA) of the gut microbiota was based on the weighted unifrac distance, and the non-metric multidimensional scaling (NMDS) of the gut microbiota was based on Bray—Curtis similarities.

M-LDA was used as a supervised method for selecting the feature which is characteristic of the label[20] (i.e., negative or positive). Provided that random vector $x=[f_1, f_2, \ldots, f_p]^T$ is of p original features (genus), its transformation can be obtained with M-LDA according to Eq. (1),

$$y_i = e_i^T x = \sum_{j=1}^{p} e_{i,j} f_j,\ i=1,2,\ldots,d \qquad \text{Eq.(1)}$$

where y_i is the i-th transformed feature, d is the number of the transformed dimensions, and e_i is the eigenvector of the i-th largest eigenvalue λ_i of matrix $S_W^{-1}S_B$ (S_W^{-1} is the inverse of within-class scatter matrix, and S_B is the between-class scatter matrix in M-LDA).

A large $|e_{i,j}|$ indicates the increased importance of the corresponding f_i. Each projection direction e_i owns the different value of the contribution C_i, and

$$C_i = \frac{\lambda_i}{\sum_j \lambda_j} \quad \text{Eq.(2)}$$

A high C_i indicates that the corresponding e_i is important, and the importance score I_j of f_j can be defined as

$$I_j = \sum_{i=1}^{d} C_i \frac{|e_{ij}|}{e_{i1}} \quad \text{Eq.(3)}$$

Therefore, original features can be graded according to the score.

Culture and administration of *D. desulfuricans*

D. desulfuricans (catalog No. ATCC 27774, American Type Culture Collection, Manassas, VA) were cultured anaerobically in Columbia Medium (hopebiol, Qingdao, CHN) at 37°C. An anaerobic chamber (Bugbox, Ruskinn, UK) containing 10% CO_2, 10% H_2, and 80% N_2 was used for all anaerobic microbiology steps. Bacterial concentration was calculated by measuring the absorbance at a wavelength of 600 nm. The strain was finally harvested through centrifugation at 3500 *g* for 10 min, washing twice with normal saline, and resuspension in sterile normal saline with a final concentration of 5×10^9 CFU mL^{-1}. Then, 0.2 mL of the solution prepared above was administered orally to the *Apoe*$^{-/-}$ mice daily. *D. desulfuricans* was heat-killed at 121°C for 15 min. The success of the heat treatment was confirmed by the absence of growth of plated heat-killed bacteria.

Quantitative analysis of the atherosclerotic lesions

The mice were sacrificed and perfused with 10 mL of PBS containing 2% EDTA. The heart and aorta were removed and fixed in 4% paraformaldehyde. The atherosclerotic burden was quantified using an en-face preparation of the whole aorta stained with Oil Red O (ORO) and the cross-sections of the aortic root. The collagen levels in the aortic root were evaluated with Masson staining. Lesion area and size were determined with ImageJ software (CHN). The results were expressed as a percentage of the lipid-accumulating lesion area to the total aortic area analyzed.

Immunofluorescence

For immunofluorescent staining, the sections of the aortic arch were rinsed in PBS, fixed in 3.7% paraformaldehyde for 20 min, and permeabilized with 0.1% Triton X-100. Slides were blocked for 1 h in 5% bovine serum albumin before incubation with macrophage-myeloid-associated antigen CD68 (Cat #: ab955, Abcam, CHN), anti-intercellular adhesion molecule 1 (ICAM-1, Cat #: sc-8439, Santa Cruz, CHN), or anti-phosphorylated-p65 (P-p65, Cat #: 3033, Cell Signaling Technology, CHN) antibodies. The section of the colon was treated with anti-zona occludens protein-1 (ZO-1, Cat #: ab221547, Abcam, CHN) or anti-Occludin (Cat #: ab216327, Abcam, CHN) at 4°C, then rinsed and incubated with FITC-conjugated secondary antibodies (Abcam, CHN) and counterstained with DAPI (Abcam, CHN).

Immunohistochemistry

The tissues were fixed in 4% paraformaldehyde (Sigma, CHN) and then cut into 4 μm sections. The aortic arch sections were incubated overnight with anti-vascular cell adhesion molecule 1 (VCAM-1, Cat #: sc-13160, Santa Cruz, CHN), anti-monocyte chemoattractant protein-1 (MCP-1, Cat #: ab155688, Abcam, CHN), or anti-TLR4 (Cat #: sc-293072, Santa Cruz, CHN) antibody, and then incubated with horseradish peroxidase-conjugated secondary antibody. The visualization of the target protein was performed using 3′3-diaminobenzidine in the presence of H_2O_2, and sections were counterstained with Harris hematoxylin. In the quantification of images, five regions were randomly collected from different regions of each section. The intensity of positive staining was analyzed with Image J software and calculated as the percentage of the total area of lesion or villa in each field.

Total RNA isolation and quantitative real-time PCR

Total RNA of aorta or colon was extracted with RNAiso reagent (Cat #: 9109, Takara, CHN). Complementary DNA was synthesized using a complementary DNA synthesis kit (Cat #: RR047A, Takara, CHN). Quantitative Real-Time PCR (qPCR) was performed on the CFX Connect apparatus (Bio-Rad, USA) with a TB Green-based real-time PCR master mix (Cat #: RR820A, Takara, CHN). The primers for each specific gene are listed in Table S1.

Measurement of serum and liver lipid content

The concentration of serum total triglyceride (TG), total cholesterol (TC), low-density lipoprotein (LDL), and high-density lipoprotein (HDL) were determined with enzymatic colorimetric assays using Chemray 240 (Rayto, CHN). Liver tissues were fixed in 4% paraformaldehyde (Cat #: 158127, Sigma, CHN) and then frozen sectioning was processed for staining with hematoxylin and eosin for microscopic examination and ORO for the assessment of hepatic fat accumulation.

Biochemical and immunological assays

The expression levels of interleukin-1β (IL-1β), interleukin-6 (IL-6), and tumor necrosis factor-alpha (TNF-α) in sera were measured by an enzyme linked immunosorbent assay with an Epoch system (BioTek, USA).

Fecal samples were collected at 24 h after the last oral gavage. Lipopolysaccharide (LPS) levels in serum, and mesenteric adipose tissue were measured with LAL assay according to a previously described protocol.[6]

For glucose tolerance assay, the mice were injected with glucose (2 g kg^{-1} body weight) intraperitoneally after fasting overnight. Blood samples were measured at 0, 30, 60, 90, and 120 min with a glucometer (Arkray, USA).

The heart, liver, spleen, lung, and kidney were examined after sacrificed and sections were stained with haematoxylin and eosin (HE) for histological analysis.

Gut permeability assay

The integrity of the intestinal barrier was investigated according to a previously described protocol.[21] Briefly, 18-week-old mice were fasted and water-deprived for 4 h and subsequently dosed by oral gavage with FITC-dextran (500 mg kg^{-1}, 4 kDa; Sigma—Aldrich, USA). After 4 h, the mice were euthanized and FITC-dextran plasma concentrations were analyzed on a fluorescence spectrophotometer (ex/em = 485/535 nm; Synergy H1, BioTek, USA).

Culture of intestinal epithelial cells

Caco-2 cells, human intestinal epithelial cells, were purchased from the American Type Culture Collection and cultured in Dulbecco's modified Eagle's medium with GlutaMax and high glucose (Thermo Fisher, CHN) supplemented with 10% heat-inactivated fetal bovine serum (Gibco, CHN), penicillin (100 U mL^{-1}; Gibico, CHN), streptomycin (100 μg mL^{-1}; Gibico, CHN), and 1 mM sodiumpyruvate (Gibco, CHN) at 37°C and 5% CO_2.[21]

Western blot

Western blot was described previously.[22] Briefly, Caco-2 cells were lysed in a lysis buffer containing protease and phosphatase inhibitors. The proteins were quantified by BCA protein assay kit (Cat #: A53226, ThermoFisher, USA) according to the manufacturer's instructions, and then fractionated by SDS-PAGE and electrophoretically transferred onto polyvinylidene fluoride membranes. The membrane was blocked with 5% skim milk for 2 h at room temperature, and then incubated with anti-GAPDH (Cat #: 60004-1-Ig, Proteintech, CHN), anti-ZO-1 (Cat #: 21773-1-AP, Proteintech, CHN) or anti-Occludin (Cat #: 27260-1-AP, Proteintech, CHN) antibodies overnight at 4°C. Finally, the protein bands were quantified using densitometry (Cat #: 1708371, Bio-Rad, USA) and Quantity One software.

TAK-242 treatment of mice

TAK-242 (10 mg) was dissolved in 1 mL of DMSO and further diluted in sterile endotoxin-free water. TAK-242 (3 mg kg^{-1} body weight) was injected intraperitoneally into the mice in an injection volume of 0.1 mL 10 g^{-1} body weight every other day.[23–25] Treatment was maintained over a 10-week period, during which body weights were recorded daily and food consumption was measured weekly.

Statistical analysis

All experiments were randomized and blinded. Statistical analyses were performed using Prism (Graphpad, v7) and SPSS (v23). Data were presented as mean ± SD. Experiments were performed with a minimum of three replications. Statistical significance was determined at $P < 0.05$ through a one-way analysis of variance with Tukey's/Dunn's multiple comparison test or Student *t*-test. Details of statistical methods and tests employed are provided in the figure legends.

Data availability

The data sets are available in the National Center for Biotechnology Information (NCBI) database under the accession number SUB9226740 (https://submit.ncbi.nlm.nih.gov/subs/sra/SUB9226740).

Results

Core gut microbes in atherosclerotic mice were identified through modified-linear discriminant analysis

To compare the gut microbial profile in non-atherosclerotic (CK) and atherosclerotic (AS) mice, 16S ribosomal RNA (16S rRNA) gene sequencing in fecal samples was performed (Fig. 1A). α-diversity indices, including the Shannon—Wiener, Simpson, and Pielou indices increased in AS mice (Fig. 1B—D). Gram-positive- to Gram-negative strain ratio also increased in AS mice (Fig. 1E).

For the analysis of the gut microbial profiles of the two groups, the samples were clustered into three clusters at the genus level according to a previous report.[26] The three clusters were classified according to the genus as follows: *Bacteroides* in cluster 1, *Prevotella* in cluster 2, and *Faecalibacterium*, *Ruminococcus*, or *Bifidobacterium* in cluster 3. The CK group was characterized with clusters 1 and 3. However, all of the samples in the AS group were categorized into cluster 3 (Fig. 1F). The PCoA and the NMDS of CK and AS showed clear separation (Fig. 1G, H), indicating that the structure of the gut microbiota in the two groups had significant differences ($P < 0.05$) and these microbes may have effects on the development of atherosclerosis. Therefore, we then used M-LDA, based on the abundance of the gut microbiota in the level of genus, to score the importance of the microbes, the top 10 genera of scores were represented as yellow columns (Fig. 1I), and the abundance was represented as a heatmap (Fig. 1I). The equations are as follows:

$$y_i = e_i^T x = \sum_{j=1}^{p} e_{i,j} f_j,\ i = 1, 2, \ldots, d \qquad \text{Eq.(1)}$$

$$C_i = \frac{\lambda_i}{\sum_j \lambda_j} \qquad \text{Eq.(2)}$$

$$I_j = \sum_{i=1}^{d} C_i \frac{|e_{ij}|}{e_{i1}} \qquad \text{Eq.(3)}$$

In the course of atherosclerotic research, we found that the high-fat-diet-induced aggravation of atherosclerosis lesion was accompanied by a marked increase in *D. desulfuricans*. Therefore, according to the score, we selected *D. desulfuricans* as the target bacterium in determining whether it affects atherosclerosis. As shown in Figure 1I, it is apparently found that the genus *Allobaculum* had higher abundance and importance than genus *Desulfovibrio*. However, it is a pity that the *Allobaculum* is unavailable for us from the DSMZ (Deutsche Sammlung von Mikroorganismen und Zellkulturen).

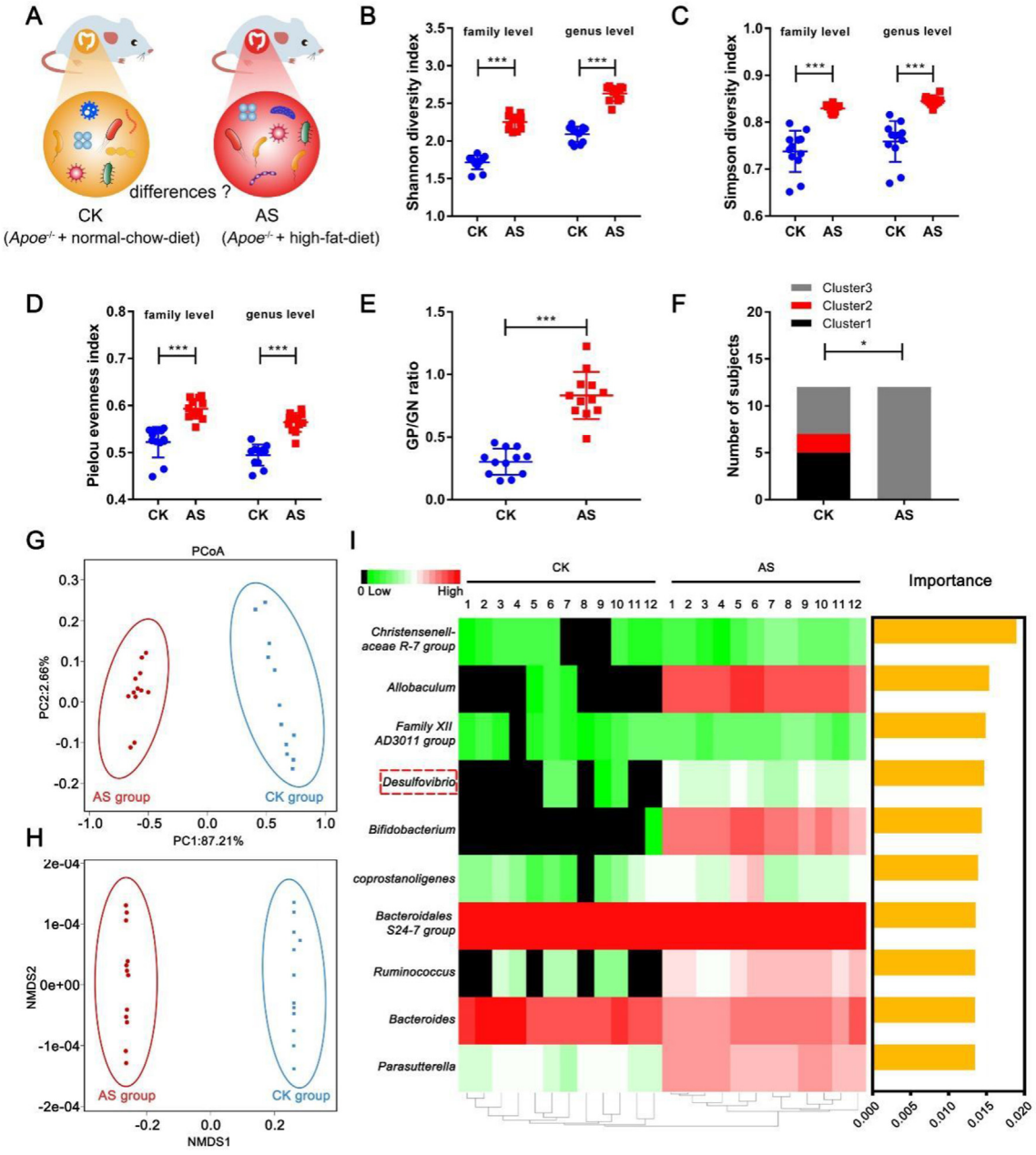

Figure 1 Differences of gut microbiota pattern between *Apoe*$^{-/-}$ mice with or without atherosclerosis. The V3—V4 region of the bacterial 16S rRNA was sequenced in fecal samples from 12 non-atherosclerotic (CK) mice and 12 atherosclerotic (AS) mice. Then, comparisons were carried out using alpha and beta diversity. **(A)** The schematic illustration of the comparison of gut microbiota between CK and AS group. **(B)** The Shannon—Wiener index at the family and genus level. **(C)** The Simpson index at the family and genus level. **(D)** The Pielou index at the family and genus level. **(E)** Gram-positive (GP) to Gram-negative (GN) strain ratio. **(F)** Distribution of each cluster in healthy mice and atherosclerotic mice. The χ^2 test was used to compare the 2 groups. **(G)** Principal coordinate analysis (PCoA) of gut microbiota based on Weighted Unifrac distance. **(H)** Non-metric multidimensional scaling (NMDS) of gut microbiota based on Bray—Curtis similarities. They illustrated the difference in the microbial composition among the samples. **(I)** Heat map with M-LDA score in the level of genus. The heat map indicates the relative percentage of each genus for the different groups. The M-LDA score means the importance of each genus that distinguished the CK and AS groups. Data are shown as mean ± SD (fecal samples $n = 12$ per group). Unpaired t test (two-tailed) was performed **(B—E)**, $P < 0.05$ (*), $P < 0.001$ (***).

Gavage with *D. desulfuricans* aggravated the formation of atherosclerotic lesion in *Apoe*$^{-/-}$ mice

To determine the effect of *D. desulfuricans* on the development of atherosclerosis, high-fat-diet *Apoe*$^{-/-}$ mice were treated with live *D. desulfuricans*, hk-*D. desulfuricans*, or PBS (vehicle) through oral gavage daily for 10 weeks, then the mice were euthanized and atherosclerotic lesions were assessed (Fig. 2A).

Compared with the high-fat-diet group, the mice gavaged with live *D. desulfuricans* showed significantly

enhanced atherosclerotic plaque area in the aorta and aortic root (Fig. 2B, C). High-fat-diet resulted in a 2.26-fold increase (Fig. 2D, aorta) and 3.19-fold increase (Fig. 2E, aortic root) in atherosclerotic lesion compared with those in normal chow diet mice, and the administration of live *D. desulfuricans* dramatically increased the lesion by 100% (Fig. 2D, aorta) and 55.7% (Fig. 2E, aortic root) in *Apoe*$^{-/-}$ mice subjected to a high-fat-diet. Furthermore, the aorta was further divided into the aortic arch, thoracic aorta, and abdominal aorta (Fig. 2D), and the size of the atherosclerotic plaque was significantly increased with the treatment of live *D. desulfuricans*. However, the mice treated with the same dose of heat-killed *D. desulfuricans* did not suffer the fate of worsening atherosclerosis, indicating that the viability of *D. desulfuricans* was indispensable for the aggravated effect. Masson staining showed a similar result, and the collagen content in the lesion area was increased after the administration of *D. desulfuricans* (Fig. S1).

To prove that the enhancement of atherosclerosis was caused by the gavage of *D. desulfuricans*, rather than the alternative composition of the gut microbiota, we detected the pattern of the gut microbiota through 16S rRNA sequencing. Compared with the normal chow diet, high-fat-diet caused a significant increase in *Actinobacteria* and *Firmicutes* and a remarkable decrease in *Bacteroidetes*, *Proteobacteria*, *Tenericutes*, and *Fusobacteria* (Fig. S2A—F). However, no significant difference was observed in the proportion of the above-mentioned bacteria among the high-fat-diet groups (Fig. S2A—F). The above results indicated that atherosclerosis was aggravated by the daily administration of *D. desulfuricans*, rather than by a change in the pattern of the gut microbiota.

Live *D. desulfuricans* exacerbated aortic and systematic inflammation

Previous studies revealed that hyperlipidemia and inflammation represent the two major pillars in the pathophysiology of atherosclerosis.[27—29] To investigate whether atherosclerosis in *Apoe*$^{-/-}$ mice was aggravated by increased inflammation, we assessed cytokines and chemokines in serum and aorta.

At a global level, the content of the proinflammatory cytokines IL-1β, IL-6, and TNF-α increased in the high-fat-diet-induced mice compared with normal chow diet mice, and the tendency was further forwarded after the administration of live *D. desulfuricans* (Fig. S3). However, the phenomenon did not occur in the mice gavaged with hk-*D. desulfuricans*.

Compared with the high-fat-diet mice, *D. desulfuricans*-treated mice had significantly more macrophages in atherosclerotic lesions, as shown by immunofluorescent staining of the macrophage-myeloid associated antigen CD68 (Fig. S4A, C, D). Similarly, the expression of VCAM-1, which is important for the recruitment of leukocytes to the sites of inflammation,[30] significantly increased after the administration of *D. desulfuricans* (Fig. S4B, E). Furthermore, the other two chemokines ICAM-1 (Fig. S5A, C, D) and MCP-1 (Fig. S5B, E) increased in *D. desulfuricans*-treated mice. We confirmed these results with qPCR, and the mRNA expression levels of F4/80, MCP-1, ICAM-1, and VCAM-1 (Fig. S6) in the aortas were upregulated in the *D. desulfuricans*-treated *Apoe*$^{-/-}$ mice.

Then, we determined whether *D. desulfuricans* had effects on lipid metabolism. Compared with the normal chow diet group, the serum levels of TG, TC, LDL, and HDL increased in the high-fat-diet groups (Fig. S7A—D). However, the administration of *D. desulfuricans* did not result in significant differences. The liver is crucial to lipid metabolism and transportation, and thus lipid accumulation in the liver was assessed by ORO staining. Compared with the normal chow diet group, the ORO-stained areas in the high-fat-diet groups dramatically increased (Fig. S7E, F). However, treatment with *D. desulfuricans* did not significantly alter lipid metabolism. We recorded fasting blood glucose and the glucose tolerance of the mice (Fig. S8A, B). The treatment of *D. desulfuricans* did not significantly affect fasting blood glucose levels or glucose tolerance. These results demonstrate that the proatherogenic effect of *D. desulfuricans* was not due to altered lipid or glucose metabolism.

The food intake and body weight of each mouse were recorded and used in monitoring the effect of *D. desulfuricans* on physiological state. Food intake and body weight slightly decreased in the *D. desulfuricans*-treated *group*, but no significant difference was observed (Fig. S8C, D). The pathological morphology of organ tissues including heart, liver, spleen, lung, and kidney were determined with HE staining, and no significant differences were observed in the morphology of the tissues treated with *D. desulfuricans* (Fig. S9).

Intestinal permeability increased in *D. desulfuricans*-aggravated atherosclerosis

LPS can suppress the cholesterol efflux of macrophages and thus promote macrophage-derived foam cell formation and atherosclerosis development.[31,32] The leaking of LPS from the gut into the circulation is regulated by the mucin layer and depends on the expression levels of the major tight junction proteins of the intestine.[5,33,34] Therefore, we detected the thickness of the mucin layer and the number of goblet cells in the colon through Alcian blue staining and the expression level of ZO-1 with immunofluorescence. High-fat-diet considerably decreases the mucin layer thickness and the number of goblet cells, and *D. desulfuricans* enhanced these effects (Fig. 3A, C, D). The expression of ZO-1, quantified using the area, was evidently downregulated after treatment with *D. desulfuricans* (Fig. 3B, E, F).

Another tight junction protein, Occludin (Fig. S10A—C), exhibited similar results. We then determined the gut barrier function according to FITC-dextran leakage from the colonic lumen to blood. As shown in (Figure S10D), *in vivo* gut permeability was significantly increased in the *D. desulfuricans*-treated mice. The expression levels of mucoprotein 3 (Muc-3), which constitutes the mucus layer, were significantly low in the *D. desulfuricans*-treated mice. The expression levels of ZO-1, Occludin, and Claudin-3, which mirror the integrity of tight junctions were also significantly decreased by high-fatdiet and further downregulated by *D. desulfuricans* (Fig. S10E).

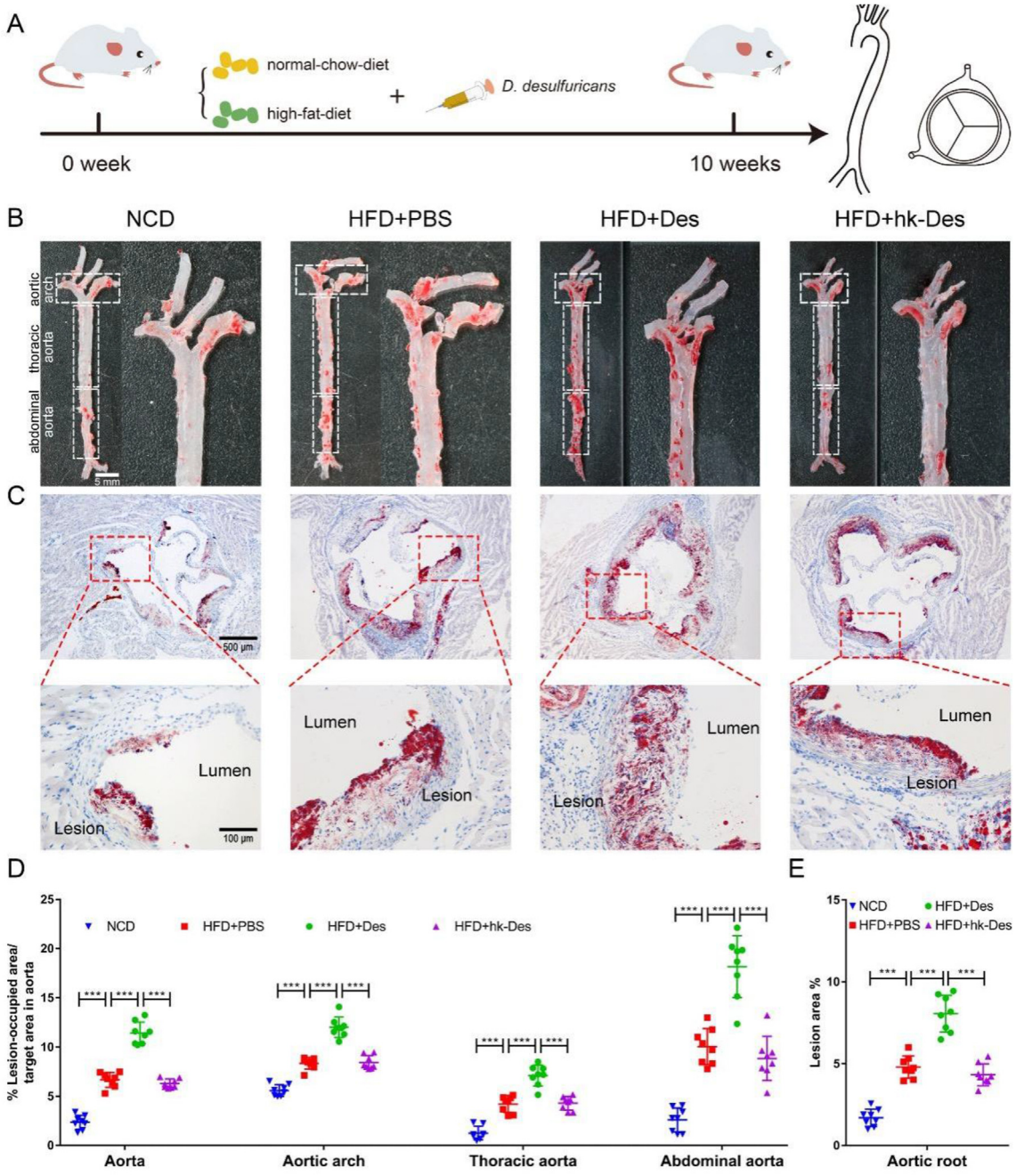

Figure 2 *D. desulfuricans* increased atherosclerotic lesions of high-fat-diet *Apoe*$^{-/-}$ mice. Eight-week-old *Apoe*$^{-/-}$mice were fed either a normal chow diet (NCD) or high-fat-diet (HFD) for 10 weeks. The high-fat-diet fed mice were further separated into 3 groups: a group gavaged with PBS as vehicle control (HFD + PBS); a group receiving daily oral gavage with live *D. desulfuricans* (HFD + Des); a group receiving daily oral gavage with heat-killed *D. desulfuricans* (HFD + hk-Des). **(A)** The schematic illustration of mice with various treatments and sampling processes. **(B)** Representative photomicrographs of Oil Red O (ORO) staining and quantitative analysis of atherosclerotic plaque areas in the aortas. **(C)** Representative photomicrographs of ORO staining and quantitative analysis of atherosclerotic plaque areas in the aortic root. **(D)** The lesion areas in the aorta, aortic arch, thoracic aorta, abdominal aorta, and **(E)** aortic root sections were analyzed by Image J software. Data are presented as mean ± SD ($n = 8$ per group). Significances among the 4 groups were determined by one-way ANOVA, followed by post hoc pairwise comparisons with the Tukey honest significant difference. $P < 0.001$ (***).

Furthermore, we performed *in vitro* studies to validate the integrity of tight junctions in intestinal cells. The Caco-2 cell line, which is derived from human colonic carcinoma and can express surface markers and tight junctions characteristic of the epithelial cell monolayer of the intestinal villus, was used in determining whether metabolites from *D. desulfuricans* affect tight junctions. The expression levels of ZO-1 and Occludin in the Caco-2 cells significantly decreased after

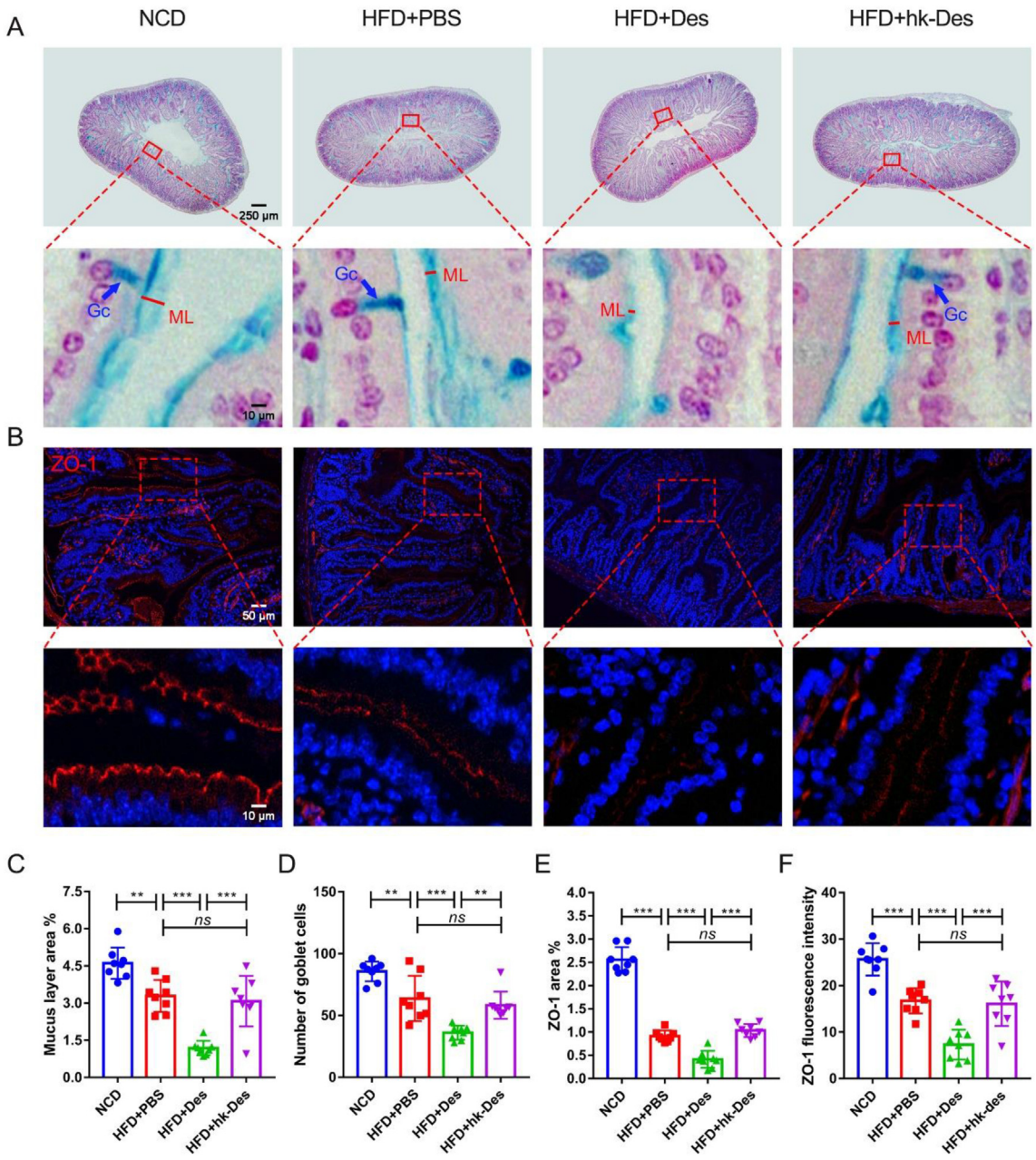

Figure 3 Intestinal permeability was increased by *D. desulfuricans* through decreasing the expression of tight junction proteins and the thickness of the mucin layer. *Apoe*$^{-/-}$ mice were grouped and treated as in Figure 2. **(A)** Mucin layer (ML) in the colon was stained with alcian blue. The thickness of the ML and the number of goblet cells (Gc) were measured to represent intestinal permeability. **(B)** Representative immunofluorescence staining for zona occludens protein-1 (ZO-1). **(C, D)** Quantity analysis of the images from **(A)** ($n = 8$ per group). **(E, F)** Quantitative analysis of images from **(B)** ($n = 8$ per group). Data are shown as mean ± SD. Significances among the 4 groups were determined by one-way ANOVA, followed by post hoc pairwise comparisons with the Tukey honest significant difference. *ns* (no significance), $P < 0.01$ (**), or $P < 0.001$ (***).

inoculation with a *D. desulfuricans* culture medium (Des IM) for 6 h (Fig. 4A—D). However, treatment with a plain inoculating medium (Plain IM) showed no significant effect. We used *Escherichia coli*, which is similar to *D. desulfuricans* and characterized as a Gram-negative bacterium, as a positive control to confirm the downregulation of the tight junction proteins of *D. desulfuricans*. Compared with the *E. coli* inoculating medium (Ecoli IM), the expression levels in Des IM significantly decreased. The same result was observed by Western blot (Fig. 4E, G), indicating that the destruction of the intestinal barrier function of *D. desulfuricans* is independent of a Gram-negative bacterium.

There have been studies showing that some gut microbes are coupled with intestinal permeability and inflammation, such as *Akkermansia muciniphila* (*AKK*), a mucin-degrading bacterium that could positively modulate the mucus thickness and gut barrier integrity.[5,35] We, therefore, compared the gut microbial composition

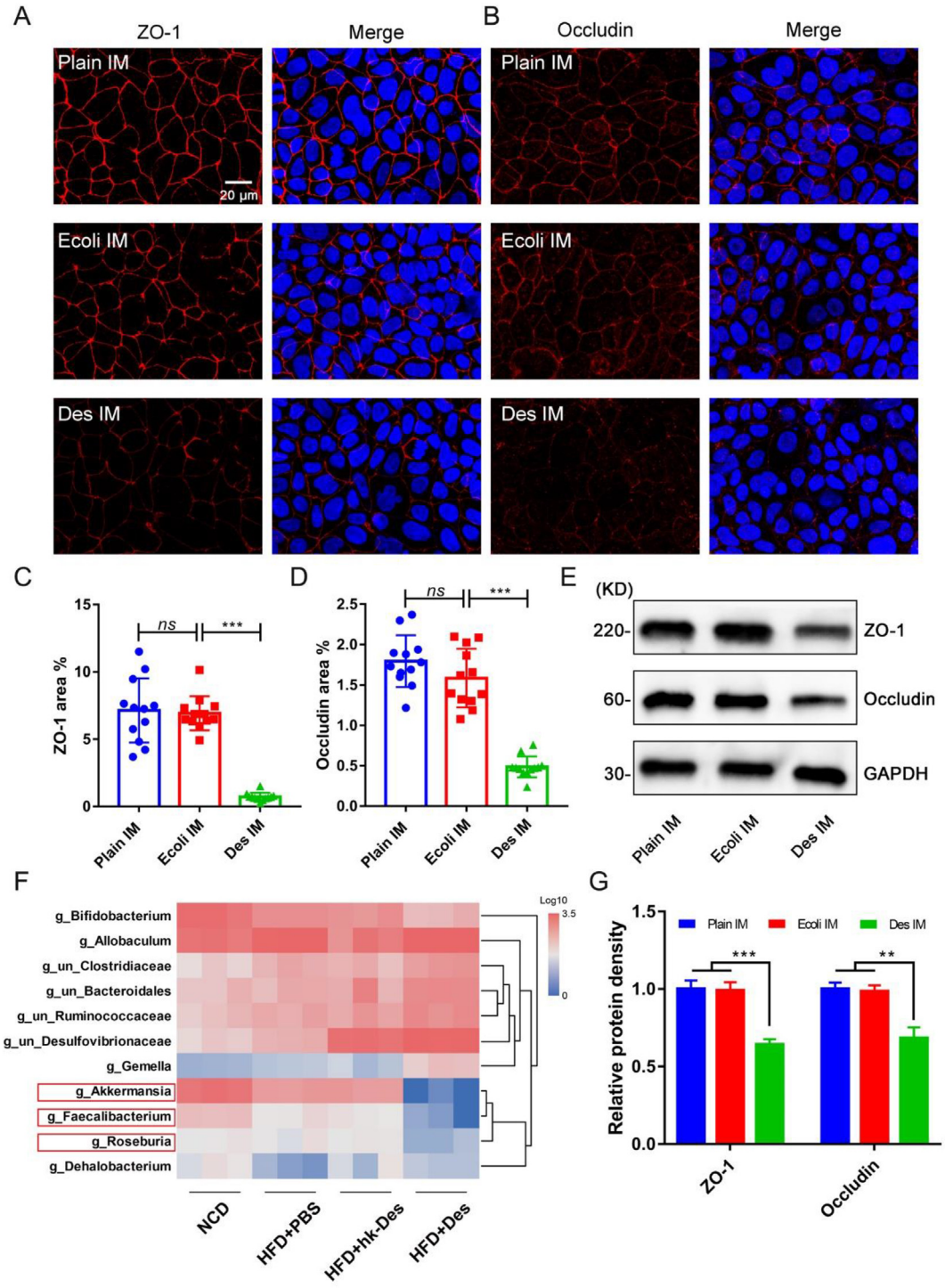

Figure 4 The expression levels of tight junction proteins were decreased in Caco-2 cells inoculated with *D. desulfuricans* culture inoculating medium. Caco-2 cells were co-cultured with plain inoculating medium (Plain IM, 100 μL/mL), *Escherichia coli* inoculating medium (Ecoli IM, 100 μL/mL), or *D. desulfuricans* culture inoculating medium (Des IM, 100 μL/mL) for 6 h. **(A)** Representative immunofluorescence staining for ZO-1. **(B)** Representative immunofluorescence staining for Occludin. **(C, D)** Quantitative analysis of images from **(A)** and **(B)** ($n = 12$ per group). **(E)** The expression of tight junctions was examined by Western blot. **(F)** Gut microbiota with statistically significant differences (HFD + PBS *vs* HFD + Des, $P < 0.05$) was represented as a heatmap. The red boxes represent intestinal-permeability protective microbes. **(G)** Western blot protein bands were quantified using densitometry and Quantity One software. Data are shown as mean ± SD. Significances among the 4 groups were determined by one-way ANOVA, followed by post hoc pairwise comparisons with the Tukey honest significant difference. *ns* (no significance), $P < 0.01$ (**), or $P < 0.001$ (***).

between HFD + PBS and HFD + Des, and microbes with statistical significance ($P < 0.05$) at the genus level were presented as a heatmap (Fig. 4F). *AKK* was decreased after treatement of *D. desulfuricans*. *Faecalibacterium prausnitzii* and *Roseburia intestinalis*, which are well-known bacteria with butyrate-producing capacity and anti-inflammatory effects,[36,37] also decreased in *D. desulfuricans*-administered mice. According to the results above, we considered that the increased-intestinal-permeability effect of *D. desulfuricans* may be caused by the disruption of intestinal-permeability protective microbes.

TAK-242 suppressed the proatherogenic effect of *D. desulfuricans*

We next detected the LPS level in serum and mesenteric adipose tissues. As shown in Figure 5A and B, the high-fat-diet-induced increases in serum LPS level and mesenteric adipose tissue LPS level were significantly enhanced in *D. desulfuricans*-treated mice but not in the hk-*D. desulfuricans* mice.

TLR4 is the receptor for LPS, and the stimulation of TLR4 activates proinflammatory pathways and induces cytokine expression in a variety of cell types.[38] Hence, the expression level of TLR4 and distribution of downstream nuclear factor-κB (NF-κB) signaling pathway-related protein P-p65, which reflects the activation of TLR4/NF-κB signaling, in the aortic root was detected. The expression of TLR4 (Fig. S11A, B) and P-p65 (Fig. 5C—E) significantly increased after treatment with *D. desulfuricans*. The mRNA expression levels of TLR4 and NF-κB in the local aortic tissues were elevated (Fig. S11C, D). The results indicate that the proatherogenic effect of *D. desulfuricans* is caused by the activation of TLR4/NF-κB signaling.

We considered that the proatherogenic effect of *D. desulfuricans* can be inhibited by blocking the recognition of TLR4 and LPS. For this purpose, TAK-242, a specific inhibitor of TLR4 that blocks the interactions between TLR4 and its adaptor molecules, was used. Eight-week-old *Apoe*$^{-/-}$ mice were treated with TAK-242 (3 mg kg^{-1} body weight) or PBS (vehicle control) for 10 weeks through intraperitoneal injection (Fig. 6A). The lesion area in the aorta and aortic root (Fig. 6B—D), and the collagen content in the aortic root were significantly reduced after the administration of TAK-242 (Fig. S12).

The serum (Fig. 7A) and mesenteric adipose tissue (Fig. 7B) LPS levels were not affected by TAK-242. However, the expression level of TLR4 (Fig. S13A, B) with immunohistochemical staining and the mRNA expression levels of TLR4 and NF-κB dramatically decreased (Fig. S13C, D). The expression level of *D. desulfuricans*-induced P-p65 increase in the aortic root significantly decreased by TAK-242 (Fig. 7C—E).

The number of infiltrated macrophages (Fig. S14A, C, D) and the levels of inflammatory molecules VCAM-1 (Fig. S14B, E), ICAM-1 (Fig. S15A, C, D), and MCP-1 (Fig. S15B, E) in the atherosclerotic lesions decreased in TAK-242-treated mice. The mRNA expression levels of F4/80, MCP-1, ICAM-1, and VCAM-1 in the aortas were downregulated after TAK-242 treatment (Fig. S16A—D). In addition, the expression levels of proinflammatory factors IL-1β, IL-6, and TNF-α (Fig. S16E—G) in the sera were attenuated by the administration of TAK-242. Fasting glucose level (Fig. S17A), glucose tolerance (Fig. S17B), food intake (Fig. S17C), body weight (Fig. S17D), lipid metabolism (Fig. S18), tissues morphology (Fig. S19), gut microbiota structure (Fig. S20), and intestinal permeability (Fig. S21, S22) were assayed. The factors were not affected by TAK-242. The results demonstrate that the proatherogenic effect of *D. desulfuricans* was enhanced after the level of circulating LPS increased and TLR4/NF-κB signaling was activated. The selective inhibitor TAK-242 has a protective effect against *D. desulfuricans*-induced atherosclerosis by blocking the recognition of TLR4 and LPS but did not change others, indicating that LPS is an important factor aggravating atherosclerosis.

Discussion

The gut microbiota can influence the development of atherosclerosis. The amplicon sequencing of 16S rRNA is widely used in estimating the composition of the gut microbiota. Although the relative abundance of the gut microbes in the samples can be compared, the "importance," alternatively called "contribution," of each microbe was hard to assess, and thus the target microbes that affect the disease were difficult to determined. Thus, we propose the use of M-LDA, a feature extraction technique, according to the relative abundance of the gut microbiota in the evaluation of the relative contribution of each microbe.

The traditional LDA method usually scores the original features only in the first dimensional projection direction of the LDA space. In M-LDA, all the divisible projection directions of LDA space are determined by setting the divisibility threshold, then the original features are scored in these directions. The overall score of each feature in the LDA space is obtained by adding these scores. Collectively, the traditional LDA method is only based on one projection direction in the evaluation of the features, and M-LDA is used in evaluating the features with all the divisible projection directions. These procedures increase the accuracy of the evaluation. The experimental results show that *D. desulfuricans* is indeed associated with atherosclerosis, indicating the validity of M-LDA.

Some specific gut microbes, such as *Akkermansia muciniphila*,[5] *Bacteroides vulgatus*, *Bacteroides dorei*,[6] and *Roseburia intestinalis*[39] are associated with the development of atherosclerosis. However, the roles of many gut bacteria in the development of atherosclerosis are still unclear because the gut microbiota constitute a complex consortium of microbial species and strains[40] and have intricate interaction with the host immune system.[41] We consider that this method, "abundance combined with importance," should be used not only in discriminating atherosclerosis associated gut microbes but also in other diseases.

Barrier dysfunction in the intestine is a pathogenic factor in *D. desulfuricans*-induced UC,[15,42] and endothelial dysfunction promotes atherosclerosis.[43,44] Here, we found that the administration of *D. desulfuricans* significantly decreased the number of goblet cells and consequently inhibited the synthesis and secretion of mucins that form the protective mucus barrier. The mucus layer is enriched with various mucins that form a hydrated gel layer covering the mucosal surface to prevent the adhesion of harmful bacteria.[5,45] Tight junctions, including Occludin, claudins, and ZOs, serve as barriers to the transepithelial influx of noxious substances/microorganisms

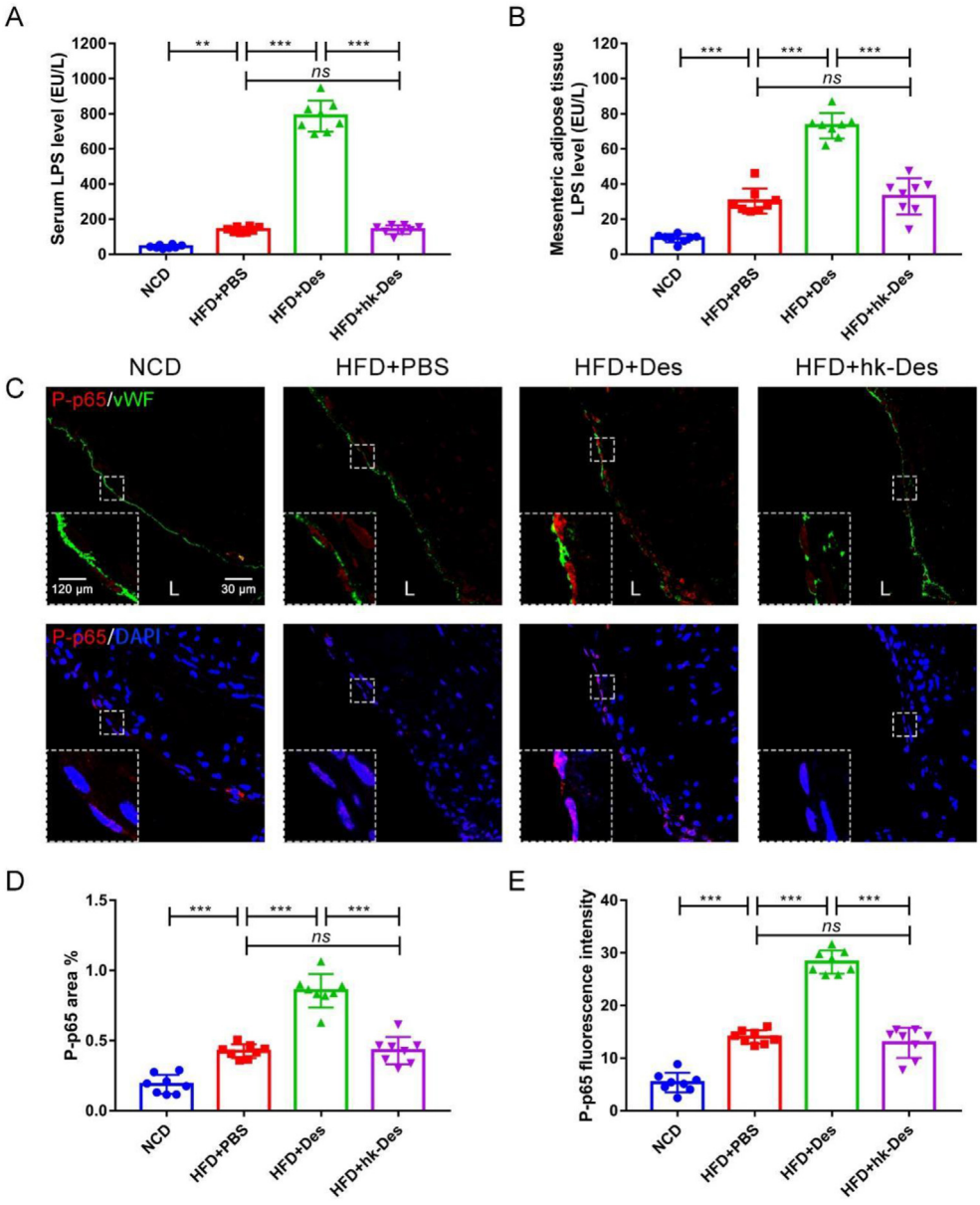

Figure 5 Local inflammation of the aortic root was increased after administration of *D. desulfuricans*. *Apoe*$^{-/-}$ mice were grouped and treated as in Figure 2. The expression of the inflammation-related proteins in atherosclerotic lesions was detected. **(A)** Serum LPS level and **(B)** mesenteric adipose tissue LPS level were measured with LAL assay. **(C)** Representative immunofluorescence staining for TLR4/NF-κB signaling pathway-related protein P-p65. **(D, E)** Quantitative analysis of images from **(C)**. Data are shown as mean ± SD ($n = 8$ per group). Significances among the 4 groups were determined by one-way ANOVA, followed by post hoc pairwise comparisons with the Tukey honest significant difference. *ns* (no significance), $P < 0.01$ (**), or $P < 0.001$ (***). L: Lumen.

from the gut lumen and are the primary control of the gut barrier.[46] ZO-1 is vital to tight junction assembly and maintenance as it can interact with other proteins, including claudins, Occludin, and actin.[47] Occludin, a transmembrane tight junction protein, can interact directly with claudins and actin.[47] Loss of Occludin and ZOs increases gut permeability.[5] The administration of *D. desulfuricans* significantly decreased the expression level of ZO-1 and Occludin in the colon of *Apoe*$^{-/-}$ mice. In addition, the expression of the two tight junction proteins in intestinal epithelial cells was inhibited after treatment with the inoculating medium of *D. desulfuricans*. These results demonstrate that the mechanism of the pro-atherogenic effect of *D. desulfuricans* is associated with gut permeability.

LPS, a potent endotoxin in the outer membrane of Gram-negative bacteria, promotes the development of balanced gut immune response.[48] Chronically low levels of circulating LPS may lead to a deleterious proinflammatory systematic immune response and are associated with the development of metabolic diseases, such as type 2 diabetes, atherosclerosis, and CVD.[48] TLR4 is a pattern-recognizing receptor that recognizes exogenous ligands, such as bacterial LPS. Evidence validated that the activation of TLR4 by LPS induces the activation of NF-κB and mitogen-activated protein kinase (MAPK) pathways and

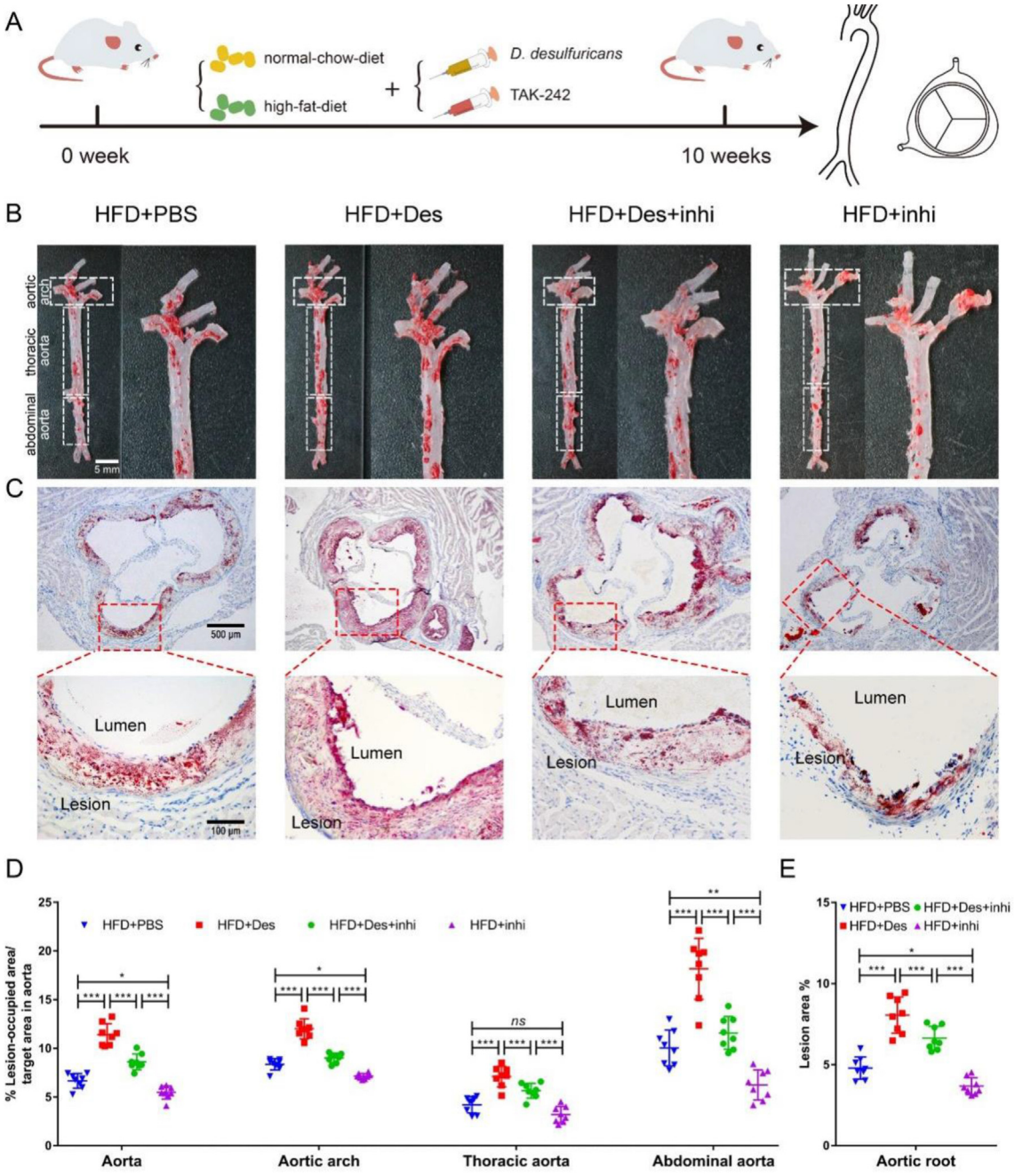

Figure 6 The proatherogenic effect of *D. Desulfuricans* was suppressed by TAK-242. Eight-week-old *Apoe*$^{-/-}$ mice were randomly assigned to four different groups, and fed with high-fat-diet for 10 weeks. A group gavaged with PBS as vehicle control (HFD + PBS); a group receiving daily oral gavage with live *D. desulfuricans* (HFD + Des); a group receiving daily oral gavage with live *D. desulfuricans* and administered intraperitoneally with TAK-242 (HFD + Des + inhi); a group receiving daily oral gavage with live PBS and administered intraperitoneally with TAK-242 (HFD + inhi). **(A)** The schematic illustration of mice with various treatments and sampling processes. **(B)** Representative photomicrographs of ORO staining and quantitative analysis of atherosclerotic plaque area in the aortas. **(C)** Representative photomicrographs of ORO staining and quantitative analysis of atherosclerotic plaque areas in the aortic root. **(D)** The lesion areas in the aorta, aortic arch, thoracic aorta, abdominal aorta, and **(E)** aortic root sections were analyzed by Image J software. Data are presented as mean ± SD ($n = 8$ per group). Significances among the 4 groups were determined by one-way ANOVA, followed by post hoc pairwise comparisons with the Tukey honest significant difference. *ns* (no significance), $P < 0.05$ (*), $P < 0.01$ (**), or $P < 0.001$ (***).

ultimately elicits the release of proinflammatory cytokines.[49] The activation of TLR4 is a key etiological condition for the development of atherosclerosis.[50]

In summary, we identified a gut bacterial species and used a model to clarify the causal relationship between *D. desulfuricans* and atherosclerosis.

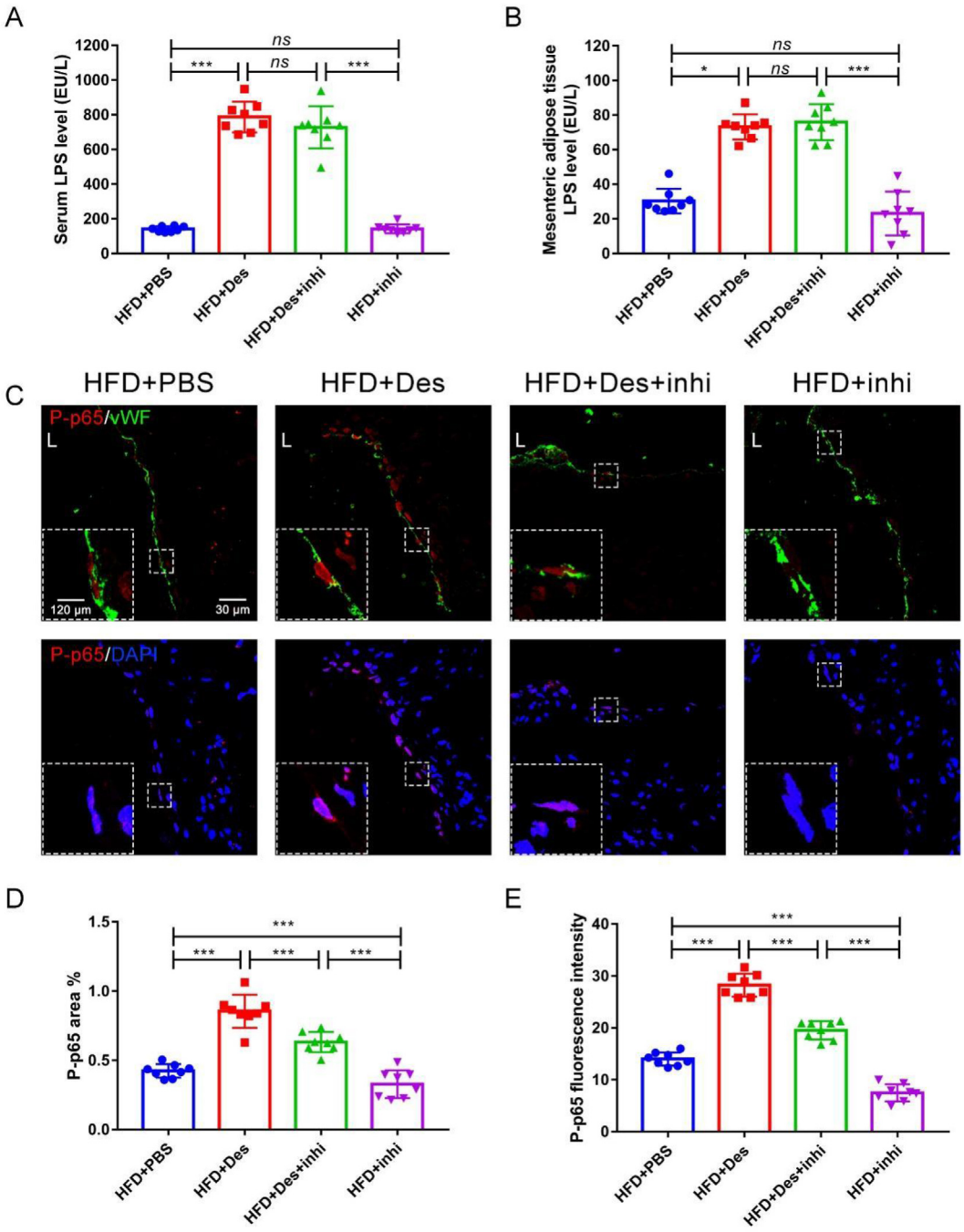

Figure 7 Local inflammation of the aortic root was decreased after administration of TAK-242. *Apoe*$^{-/-}$ mice were grouped and treated as in Figure 6. The expression of the inflammation-related proteins in atherosclerotic lesions was detected. **(A)** Serum LPS level and **(B)** mesenteric adipose tissue LPS level were measured with LAL assay. **(C)** Representative immunofluorescence staining for TLR4/NF-κB signaling pathway-related protein P-p65. **(D, E)** Quantitative analysis of images from **(C)**. Data are shown as mean ± SD ($n = 8$ per group). Significances among the 4 groups were determined by one-way ANOVA, followed by post hoc pairwise comparisons with the Tukey or Dunn honest significant difference. *ns* (no significance), $P < 0.05$ (*), $P < 0.001$ (***). L: Lumen.

Conclusion

Our results demonstrate that *D. desulfuricans* can enhance the development of atherosclerosis by increasing intestinal permeability and host inflammatory response. This work uncovered a key link among gut microbiota, gut permeability, inflammatory, and vascular system, which may improve our understanding of the progression of cardiovascular diseases.

Author contributions

K.Z., X.Q., J.H.Q., and G.X.W. designed the study. T.S. did the bioinformatic analyses. K.Q., W.H.Y., and T.H.L.

conducted animal experiments. K.Z., X.Q. and J.H.Q., drafted the first versions. K.Z., X.Q., A.U.D., Y.D.C., W.G., X.C.R. contributed to text revision and discussion. G.X.W. and J.H.Q. contributed to the manuscript review, editing, fund acquisition and supervision.

Conflict of interests

The author declares no conflict of interests.

Funding

This work was supported by grants from the National Natural Science Foundation of China (No. 12032007 and 31971242), the Chongqing Research Program of Basic Research and Frontier Technology, China (No. cstc2019jcyj-zdxmX0028), Chongqing Municipal Education Commission, China (No. KYYJ202001), and Fundamental Research Funds for the Central Universities (No. 2019CDYGZD008).

Acknowledgements

The author would like to thank Professor Mingxing Lei, Dr. Yuan Zhu, Adil Hassan, Ms. Yuan Zhong and all other members of Professor Guixue Wang's laboratory for their constructive discussions and support for the daily experimental work as well as the support from the Public Experiment Center of State Bioindustrial Base (Chongqing), China.

Appendix A. Supplementary data

Supplementary data to this article can be found online at https://doi.org/10.1016/j.gendis.2021.09.007.

References

1. Herrington W, Lacey B, Sherliker P, et al. Epidemiology of atherosclerosis and the potential to reduce the global burden of atherothrombotic disease. *Circ Res*. 2016;118(4):535–546.
2. Li T, Safitri M, Zhang K, et al. Downregulation of G3BP2 reduces atherosclerotic lesions in ApoE -/- mice. *Atherosclerosis*. 2020; 310:64–74.
3. Wang Y, Zhang K, Qin X, et al. Biomimetic nanotherapies: red blood cell based core–shell structured nanocomplexes for atherosclerosis management. *Adv Sci*. 2019;6(12), e1900172.
4. Carreras A, Bäckhed F. 23, 22 Calling the microbiota to control atherosclerosis. *Immunity*. 2018;49(5):788–790.
5. Li J, Lin S, Vanhoutte PM, et al. Akkermansia Muciniphila protects against atherosclerosis by preventing metabolic endotoxemia-induced inflammation in Apoe-/- mice. *Circulation*. 2016;133(24):2434–2446.
6. Yoshida N, Emoto T, Yamashita T, et al. Bacteroides vulgatus and Bacteroides dorei reduce gut microbial lipopolysaccharide production and inhibit atherosclerosis. *Circulation*. 2018; 138(22):2486–2498.
7. Hassan A, Din AU, Zhu Y, et al. Anti-atherosclerotic effects of Lactobacillus plantarum ATCC 14917 in ApoE-/- mice through modulation of proinflammatory cytokines and oxidative stress. *Appl Microbiol Biotechnol*. 2020;104(14):6337–6350.
8. Zhu Y, Li T, Din AU, et al. Beneficial effects of Enterococcus faecalis in hypercholesterolemic mice on cholesterol transportation and gut microbiota. *Appl Microbiol Biotechnol*. 2019;103(7):3181–3191.
9. Din AU, Hassan A, Zhu Y, et al. Amelioration of TMAO through probiotics and its potential role in atherosclerosis. *Appl Microbiol Biotechnol*. 2019;103(23–24):9217–9228.
10. Kushkevych I, Vítězová M, Vítěz T, et al. A new combination of substrates: biogas production and diversity of the methanogenic microorganisms. *Open Life Sci*. 2018;13:119–128.
11. Kushkevych I, Dordević D, Kollar P, et al. Hydrogen sulfide as a toxic product in the small-large intestine axis and its role in IBD development. *J Clin Med*. 2019;8(7), e1054.
12. Jia W, Whitehead RN, Griffiths L, et al. Diversity and distribution of sulphate-reducing bacteria in human faeces from healthy subjects and patients with inflammatory bowel disease. *FEMS Immunol Med Microbiol*. 2012;65(1): 55–68.
13. Vita N, Hatchikian EC, Nouailler M, et al. Disulfide bond-dependent mechanism of protection against oxidative stress in pyruvate-ferredoxin oxidoreductase of anaerobic Desulfovibrio bacteria. *Biochemistry*. 2008;47(3):957–964.
14. Rowan F, Docherty NG, Murphy M, et al. Desulfovibrio bacterial species are increased in ulcerative colitis. *Dis Colon Rectum*. 2010;53(11):1530–1536.
15. Duffy M, O'Mahony L, Coffey JC, et al. Sulfate-reducing bacteria colonize pouches formed for ulcerative colitis but not for familial adenomatous polyposis. *Dis Colon Rectum*. 2002;45(3): 384–388.
16. Qin J, Li Y, Cai Z, et al. A metagenome-wide association study of gut microbiota in type 2 diabetes. *Nature*. 2012;490(7418): 55–60.
17. Figueiredo MC, Lobo SA, Sousa SH, et al. Hybrid cluster proteins and flavodiiron proteins afford protection to Desulfovibrio vulgaris upon macrophage infection. *J Bacteriol*. 2013; 195(11):2684–2690.
18. Treder MS, Porbadnigk AK, et al. The LDA beamformer: optimal estimation of ERP source time series using linear discriminant analysis. *Neuroimage*. 2016;129:279–291.
19. Weber L, DeForce E, Apprill A. Optimization of DNA extraction for advancing coral microbiota investigations. *Microbiome*. 2017;5(1), e18.
20. Sáenz JS, Marques TV, Barone RSC, et al. Oral administration of antibiotics increased the potential mobility of bacterial resistance genes in the gut of the fish Piaractus mesopotamicus. *Microbiome*. 2019;7(1), e24.
21. van Rijn JM, Ardy RC, Kuloğlu Z, et al. Intestinal failure and aberrant lipid metabolism in patients with DGAT1 deficiency. *Gastroenterology*. 2018;155(1):130–143.
22. Li H, Yang F, Hu A, et al. Therapeutic targeting of circ-CUX1/EWSR1/MAZ axis inhibits glycolysis and neuroblastoma progression. *EMBO Mol Med*. 2019;11(12), e10835.
23. Abdul Y, Abdelsaid M, Li W, et al. Inhibition of Toll-like receptor-4 (TLR-4) improves neurobehavioral outcomes after acute ischemic stroke in diabetic rats: possible role of vascular endothelial TLR-4. *Mol Neurobiol*. 2019;56(3):1607–1617.
24. Chen T, Li Q, Wu J, et al. Fusobacterium nucleatum promotes M2 polarization of macrophages in the microenvironment of colorectal tumours via a TLR4-dependent mechanism. *Cancer Immunol Immunother*. 2018;67(10):1635–1646.
25. Moser VA, Uchoa MF, Pike CJ. TLR4 inhibitor TAK-242 attenuates the adverse neural effects of diet-induced obesity. *J Neuroinflammation*. 2018;15(1), e306.
26. Arumugam M, Raes J, Pelletier E, et al. Enterotypes of the human gut microbiome. *Nature*. 2011;473(7346):174–180.
27. Oliver Soehnlein. Multiple roles for neutrophils in atherosclerosis. *Circ Res*. 2012;110(6):875–888.
28. Libby P, Ridker PM, Hansson GK. Progress and challenges in translating the biology of atherosclerosis. *Nature*. 2011; 473(7347):317–325.

29. Hoeke G, Kooijman S, Boon MR, et al. Role of Brown fat in lipoprotein metabolism and atherosclerosis. *Circ Res*. 2016; 118(1):173—182.
30. Basurto L, Gregory MA, Hernández SB, et al. Monocyte chemoattractant protein-1 (MCP-1) and fibroblast growth factor-21 (FGF-21) as biomarkers of subclinical atherosclerosis in women. *Exp Gerontol*. 2019;124, e110624.
31. Zhou Y, Chen R, Liu D, et al. Asperlin inhibits LPS-evoked foam cell formation and prevents atherosclerosis in ApoE-/- mice. *Mar Drugs*. 2017;15(11), e358.
32. Majdalawieh A, Ro HS. LPS-induced suppression of macrophage cholesterol efflux is mediated by adipocyte enhancer-binding protein 1. *Int J Biochem Cell Biol*. 2009;41(7):1518—1525.
33. Cani PD, Amar J, Iglesias MA, et al. Metabolic endotoxemia initiates obesity and insulin resistance. *Diabetes*. 2007;56(7): 1761—1772.
34. Zarepour M, Bhullar K, Montero M, et al. The mucin Muc2 limits pathogen burdens and epithelial barrier dysfunction during Salmonella enterica serovar Typhimurium colitis. *Infect Immun*. 2013;81(10):3672—3683.
35. Zhou K. Strategies to promote abundance of Akkermansia muciniphila, an emerging probiotics in the gut, evidence from dietary intervention studies. *J Funct Foods*. 2017;33:194—201.
36. Sokol H, Pigneur B, Watterlot L, et al. Faecalibacterium prausnitzii is an anti-inflammatory commensal bacterium identified by gut microbiota analysis of Crohn disease patients. *Proc Natl Acad Sci U S A*. 2008;105(43):16731—16736.
37. La Rosa SL, Leth ML, Michalak L, et al. The human gut Firmicute Roseburia intestinalis is a primary degrader of dietary β-mannans. *Nat Commun*. 2019;10(1), e905.
38. Shi H, Kokoeva MV, Inouye K, et al. TLR4 links innate immunity and fatty acid-induced insulin resistance. *J Clin Invest*. 2006; 116(11):3015—3025.
39. Kasahara K, Krautkramer KA, Org E, et al. Interactions between Roseburia intestinalis and diet modulate atherogenesis in a murine model. *Nat Microbiol*. 2018;3(12):1461—1471.
40. De Filippis F, Pellegrini N, Laghi L, et al. Unusual sub-genus associations of faecal Prevotella and Bacteroides with specific dietary patterns. *Microbiome*. 2016;4(1), e57.
41. Dai M, Liu Y, Chen W, et al. Rescue fecal microbiota transplantation for antibiotic-associated diarrhea in critically ill patients. *Crit Care*. 2019;23(1), e324.
42. Katinios G, Casado-Bedmar M, Walter SA, et al. Increased colonic epithelial permeability and mucosal eosinophilia in ulcerative colitis in remission compared with irritable bowel syndrome and health. *Inflamm Bowel Dis*. 2020;26(7):974—984.
43. Mundi S, Massaro M, Scoditti E, et al. Endothelial permeability, LDL deposition, and cardiovascular risk factors-a review. *Cardiovasc Res*. 2018;114(1):35—52.
44. Phinikaridou A, Andia ME, Passacquale G, et al. Noninvasive MRI monitoring of the effect of interventions on endothelial permeability in murine atherosclerosis using an albumin-binding contrast agent. *J Am Heart Assoc*. 2013;2(5), e000402.
45. Johansson ME, Phillipson M, Petersson J, et al. The inner of the two Muc2 mucin-dependent mucus layers in colon is devoid of bacteria. *Proc Natl Acad Sci U S A*. 2008;105(39):15064—15069.
46. Pongkorpsakol P, Buasakdi C, Chantivas T, et al. An agonist of a zinc-sensing receptor GPR39 enhances tight junction assembly in intestinal epithelial cells via an AMPK-dependent mechanism. *Eur J Pharmacol*. 2019;842:306—313.
47. Turner JR. Intestinal mucosal barrier function in health and disease. *Nat Rev Immunol*. 2009;9(11):799—809.
48. Gnauck A, Lentle RG, Kruger MC. The characteristics and function of bacterial lipopolysaccharides and their endotoxic potential in humans. *Int Rev Immunol*. 2016;35(3):189—218.
49. Yang L, Guo H, Li Y, et al. Oleoylethanolamide exerts anti-inflammatory effects on LPS-induced THP-1 cells by enhancing PPARα signaling and inhibiting the NF-κB and ERK1/2/AP-1/STAT3 pathways. *Sci Rep*. 2016;6, e34611.
50. Park SJ, Lee AN, Back SK, et al. Suppression of TRIF-dependent signaling pathway of Toll-like receptors by oak wood vinegar in RAW264.7 macrophages. *Mol Cell Toxicol*. 2010;6:73—78.